nature communications

Article

https://doi.org/10.1038/s41467-024-50970-1

High-sensitive sensory neurons exacerbate rosacea-like dermatitis in mice by activating γδ T cells directly

Received: 30 October 2023

Accepted: 26 July 2024

Published online: 23 August 2024

Check for updates

Yiya Zhang[1,2,3,7], Tao Li[1,2,7], Han Zhao[1,2], Xin Xiao[1,2], Ximin Hu[1,2], Ben Wang[1,2], Yingxue Huang[1,2], Zhinan Yin[4,5], Yun Zhong[1,2], Yangfan Li[1,2,6] ✉ & Ji Li[1,2,3] ✉

Rosacea patients show facial hypersensitivity to stimulus factors (such as heat and capsaicin); however, the underlying mechanism of this hyperresponsiveness remains poorly defined. Here, we show capsaicin stimulation in mice induces exacerbated rosacea-like dermatitis but has no apparent effect on normal skin. Nociceptor ablation substantially reduces the hyperresponsiveness of rosacea-like dermatitis. Subsequently, we find that γδ T cells express Ramp1, the receptor of the neuropeptide CGRP, and are in close contact with these nociceptors in the skin. γδ T cells are significantly increased in rosacea skin lesions and can be further recruited and activated by neuron-secreted CGRP. Rosacea-like dermatitis is reduced in T cell receptor δ-deficient ($Tcrd^{-/-}$) mice, and the nociceptor-mediated aggravation of rosacea-like dermatitis is also reduced in these mice. In vitro experiments show that CGRP induces IL17A secretion from γδ T cells by regulating inflammation-related and metabolism-related pathways. Finally, rimegepant, a CGRP receptor antagonist, shows efficacy in the treatment of rosacea-like dermatitis. In conclusion, our findings demonstrate a neuron-CGRP-γδT cell axis that contributes to the hyperresponsiveness of rosacea, thereby showing that targeting CGRP is a potentially effective therapeutic strategy for rosacea.

Rosacea is a common chronic inflammatory cutaneous disease, with worldwide incidences as high as 22%[1,2]. Recent epidemiological studies have reported a significant psychological disease burden and decreased quality of life in patients with rosacea[3]. Although the specific pathogenesis of rosacea is not yet clear, clinical observations suggest that hyperresponsive nerves play a key role in the onset of rosacea. Trigger factors (such as heat and spicy food) can directly activate cutaneous sensory neurons and thereby induce immune dysregulation, leading to the manifestation of rosacea lesions[4]. However, the specific immunoregulatory mechanism of sensory neurons in rosacea is not yet clear, and there is a lack of clinical treatments for neuroimmune imbalances in rosacea.

The skin is densely innervated by multiple types of neurons, including sensory and sympathetic nerves, which cooperate with immune cells to amplify immunopathology in various skin disorders, including psoriasis[5], contact hypersensitivity[6] and infection[7]. The nerve fibers in skin are often in close proximity to immune cells. Upon activation, these neurons release mediators (including neuropeptide, neurotransmitters, inflammatory factor) locally to modulate the activity and infiltration of immune cells present in the damaged skin[8–10]. The

[1]Department of Dermatology, Xiangya Hospital, Central South University, Changsha, China. [2]Hunan key laboratory of aging biology, Xiangya Hospital, Central South University, Changsha, China. [3]National Clinical Research Center for Geriatric Disorders, Xiangya Hospital, Central South University, Changsha, Hunan, P.R. China. [4]Guangdong Provincial Key Laboratory of Tumor Interventional Diagnosis and Treatment, Zhuhai Institute of Translational Medicine Zhuhai People's Hospital Affiliated with Jinan University, Jinan University, Zhuhai, Guangdong, China. [5]The Biomedical Translational Research Institute, Health Science Center (School of Medicine), Jinan University, Guangzhou, Guangdong, China. [6]Department of Dermatology, The First Affiliated Hospital of Zhengzhou University, Zhengzhou, Henan, China. [7]These authors contributed equally: Yiya Zhang, Tao Li. ✉e-mail: yangfanli@126.com; liji_xy@csu.edu.cn

sensory fibers, most of which express markers of nociceptors, including TRPV1 and Nav1.8 channels, can be activated by a wide variety of stimuli including chemical, or thermal stimuli (heat, capsaicin). Upon external stimulation, the nerve terminals of nociceptors release neuropeptides locally, including calcitonin-gene-related peptide (CGRP, encoded by *Calca*) and substance P (SP, encoded by *Tac1*), which subsequently either amplify or inhibit the downstream inflammatory cascade by modulating the activity of immune or vascular cells[11]. Although emerging clinical observations imply the central role of neuroimmune interactions, it remains unclear whether activated sensory nerves trigger rosacea and worsen symptoms by secreting neuropeptides. Although emerging studies have revealed the upregulation and important role of neuropeptides in rosacea, their functions in modulating immune responses in rosacea remain to be explored.

Tissue-resident type 3 cytokine (IL17 and IL22)-producing T cells are prototypic innate T cells that serve critical functions in skin, lung, and adipose tissue homeostasis. In naïve mice, γδ T cells is the primary subset of T cells in the epidermis and called dendritic epidermal T cells (DETCs) due to their dendritic morphology, playing an important role in the skin barrier, wound healing, clearing of infections, tumor surveillance, and responses to allergens[12–14]. In addition, γδ T cells exist in both human and murine dermis. Dermal γδ T cells are the major IL17A–producing lymphocyte subset within the skin both at steady state and during various infections and inflammatory diseases[15]. Studies have shown that dermal IL17-producing γδ T (γδT17) cells are greatly increased in the skin lesions of psoriasis patients and IMQ-induced psoriatic mice, and play a central role in the pathogenesis of psoriasis by secreting IL17[16]. Recently, some studies revealed the link between sensory nerves and γδ T cells. Baral et al. demonstrated that isolated cutaneous TRPV1$^+$ neuron activation is sufficient to induce expansion of IL17 in TCRγδ T cells[17]. In psoriasis, neurons that induced the secretion of IL23 from DCs are essential for the subsequent recruitment and activation of dermal γδT17 cells[5]. Although IL17 immunostaining was evidently increased in rosacea patients[18], the role of γδ T cells, especially dermal IL17-producing γδ T (γδT17) cells, in rosacea remains unclear.

In this study, we describe nerve-sensitive rosacea-like skin in which nociceptor neurons were activated by capsaicin (rosacea-related stimulus factor) and then exacerbated disease severity by releasing CGRP. Furthermore, we found that γδ T cells are target cells of activated nerves, play a central role in the pathogenesis of rosacea and are further activated by CGRP, thereby resulting in exacerbated disease severity.

Results

Rosacea-like mice is highly sensitive to capsaicin stimulation

Although several studies have demonstrated the important role of sensory neurons in the pathogenesis of rosacea, our previous work[19] and Supplementary Fig. S1 show that both sensory neurons and sympathetic nerves ablation did not significant influence LL37-induced skin inflammation in mice. Next, we detected the distribution of sensory nerves in skin by analyzing the confocal micrographs of whole-mount mouse skin and we assessed the activation of sensory nerves in the dorsal root ganglia (DRG) by monitoring the expression of activating transcription factor 3 (ATF3), a transcription factor that is used as a marker for neuronal injury and activation[20]. Compared with wild-type mice, there was no significant difference in innervation density in the skin of LL37-induced rosacea-like mice (Supplementary Fig. S2A). The immunofluorescence staining revealed a slight increase of ATF3$^+$ neurons in DRG of rosacea-like mice (Supplementary Fig. S2B). These results indicated that although neurons were activated in rosace-like mice, its activation was insufficient to influence rosacea-like dermatitis.

Given that rosacea could be triggered or exacerbated by sensory nerve activation, LL37-induced rosacea-like mice were treated with capsaicin, a selective TRPV1 agonist and a stimulating factor of rosacea, to simulate hypersensitive rosacea skin in vivo. As shown in Supplementary Fig. S2B, ATF3 expression was further induced by capsaicin in rosacea-like mice. In rosacea-like mice, capsaicin administration further increased the redness score, area of erythema, and skin thickness (Fig. 1A and B). Elevated inflammation, the expression of rosacea-characteristic factors, the infiltration of CD4$^+$ T cells and the number of CD31$^+$ vessels were further induced by capsaicin treatment in LL37-induced rosacea-like dermatitis (Fig. 1C–E and Supplementary Fig. S3). However, capsaicin treatment alone did not induce erythema or inflammation in control mice (PBS control group) (Fig. 1). We conclude that consistent with rosacea patients, LL37-induced rosacea-like skin is hypersensitive to capsaicin stimulation.

Sensory nerve ablation prevents hyperresponsiveness in rosacea-like skin

Given the role of capsaicin in the activation of sensory nerves and other non-nerve cells, we used sensory nerve ablation mice to investigate the role of nerve activation in capsaicin-induced aggravation of rosacea-like dermatitis. In comparison with DMSO-treated mice, RTX-treated mice exhibited overall reduced disease activity, as reflected by evidently reduced erythema and skin thickness (Fig. 2A–C). Furthermore, histological examination of the skin revealed that the RTX-treated mice exhibited less severe histopathological changes, including reduced inflammatory cell infiltration, attenuated expression of rosacea-characteristic factors, and significantly reduced numbers of CD4$^+$ T cells and CD31$^+$ vessels (Fig. 2D–E and Supplementary Fig. S4). Next, we silenced neurons in rosacea-like mice using QX314, a charged sodium channel inhibitor. As shown in Supplementary Fig. S5A–C, pretreatment with QX314 (100 μM) reduced capsaicin-induced increases in ATF3$^+$ cells in DRGs. Macroscopic analysis also revealed that the greater redness and skin thickness induced by capsaicin in rosacea-like mice was attenuated by QX314 (Fig. 2F–J and Supplementary Fig. S4). The expression of Atf3 and the number of ATF3$^+$ cells were also reduced in RTX-treated mice and QX314-treated mice (Supplementary Fig. S5A–C).

We then bred *Nav1.8-Cre* mice with *Rosa26-DTR* mice to generate mice lacking Nav1.8$^+$ nociceptors (Nav1.8^{DTR} mice). As shown in Supplementary Fig. S6, Nav1.8^{DTR} mice (with ablated nociceptors) showed decreased ATF3 expression. In WT mice (Nav1.8^{DTR} littermate control mice, with intact nociceptors), capsaicin stimulation aggravated rosacea-like dermatitis, including erythema, skin thickness, inflammation and immune infiltration. In contrast, capsaicin-stimulated Nav1.8^{DTR} mice (with ablated nociceptors) showed significantly dampened rosacea-like dermatitis (Fig. 3).

In conclusion, the above findings clearly demonstrate that the activation of nociceptors is indispensable for the sensitivity of rosacea to capsaicin.

CGRP is required for nociceptor activation-exacerbated dermatitis

Activated sensory nerves affect surrounding cells by releasing neuropeptides[8]. To determine the neuropeptide that drives exacerbated dermatitis, we investigated the expression of neuropeptides in DRGs extracted from rosacea-like mice. As shown in Supplementary Fig. S7A, the mRNA levels of CGRP and PACAP were slightly increased in the DRGs of LL37-induced rosacea-like mice compared to the control group. Moreover, the expression of CGRP was evidently upregulated by capsaicin stimulation and reduced by sensory nerve ablation in the DRG of rosacea-like mice (Supplementary Fig. S7B and C). Although CGRP mRNA was detectable in the skin, its expression levels were much lower than those in the DRG (Supplementary Fig. S7D). In addition, it has been reported that CGRPβ is expressed by keratinocytes, while CGRPα subtype plays a role as neurotransmitter. These data strongly suggest that CGRP is transcribed mainly in DRG neuron cell bodies, and that CGRP is released into the skin through nerve endings. Next, we assessed the expression of CGRP in the skin of rosacea. Confocal microscopy of skin samples showed co-staining of

https://doi.org/10.1038/s41467-024-50970-1

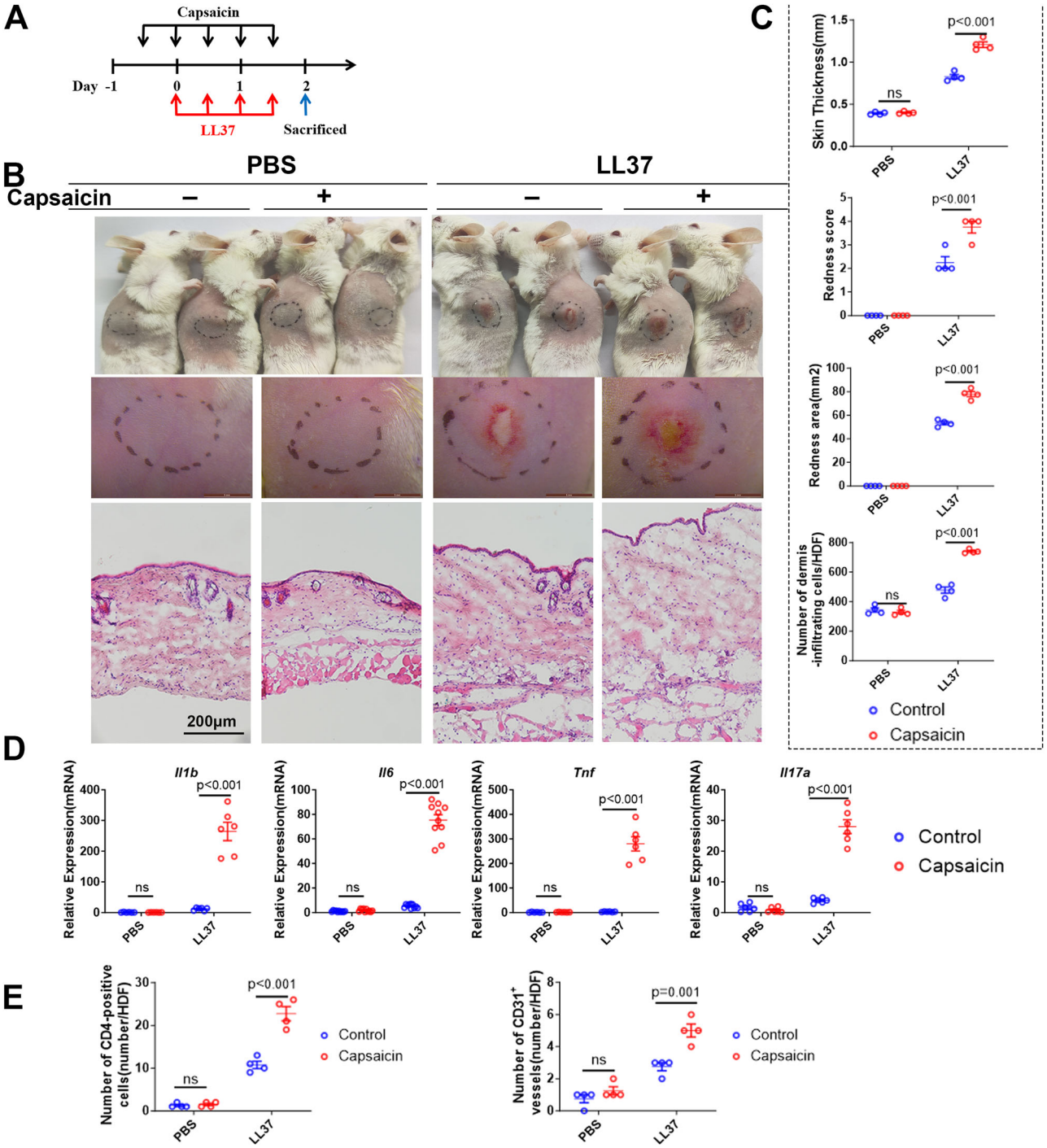

Fig. 1 | Nociceptor activation promotes rosacea-like dermatitis. A Diagram of the experimental paradigm in (**A**–**E**). capsaicin or vehicle on day −1 before intradermal injection of PBS or LL37 in mice. B, Representative macroscopic images and HE-stained sections of skin tissues. **C** The redness score, area of erythema and skin thickness of skin tissues ($n = 4$ mice for each group). The mRNA levels of rosacea-characteristic factors (**D**) ($n = 6$ mice for each group), the $CD4^+$ T cells infiltration and $CD31^+$ microvasculature (**E**) ($n = 4$ mice for each group) in the skin of vehicle- or capsaicin-treated mice after LL37/PBS injection. **C**–**E** Data represent the mean ± SEM. ns, $p > 0.05$. Two--way ANOVA test was used, with Bonferroni's post hoc test.

CGRP and $Nav1.8^+$ nerves, revealing that the vast majority of CGRP was expressed by $Nav1.8^+$ nerves (Fig. 4A and Supplementary Fig. S7E). Moreover, a significant increase in CGRP expression was observed in the skin of rosacea patients compared to the skin of healthy volunteer (Fig. 4B). Although no significant increase of CGRP expression was observed in the nerves of LL37-induced rosacea-like dermatitis, capsaicin stimulation evidently increased CGRP expression in the nerves of the skin (Supplementary Fig. S7E). Consistently, we observed less CGRP in the skin from QX314 sensory nerve ablation mice compared with control littermates (Supplementary Fig. S7F). These results indicated that capsaicin-activated mouse model was more similar to the clinical phenotype of rosacea.

Next, we used $CGRP_{8\text{-}37}$, a CGRP inhibitor, to investigate the role of CGRP in capsaicin-mediated dermatitis aggravation. As expected, $CGRP_{8\text{-}37}$ treatment attenuated capsaicin-mediated dermatitis aggravation to a similar extent to that in mice with nerve denervation (Fig. 4C–G and Supplementary Fig. S8). Moreover, $CGRP_{8\text{-}37}$ treatment did not affect LL37-induced rosacea-like dermatitis (Supplementary

https://doi.org/10.1038/s41467-024-50970-1

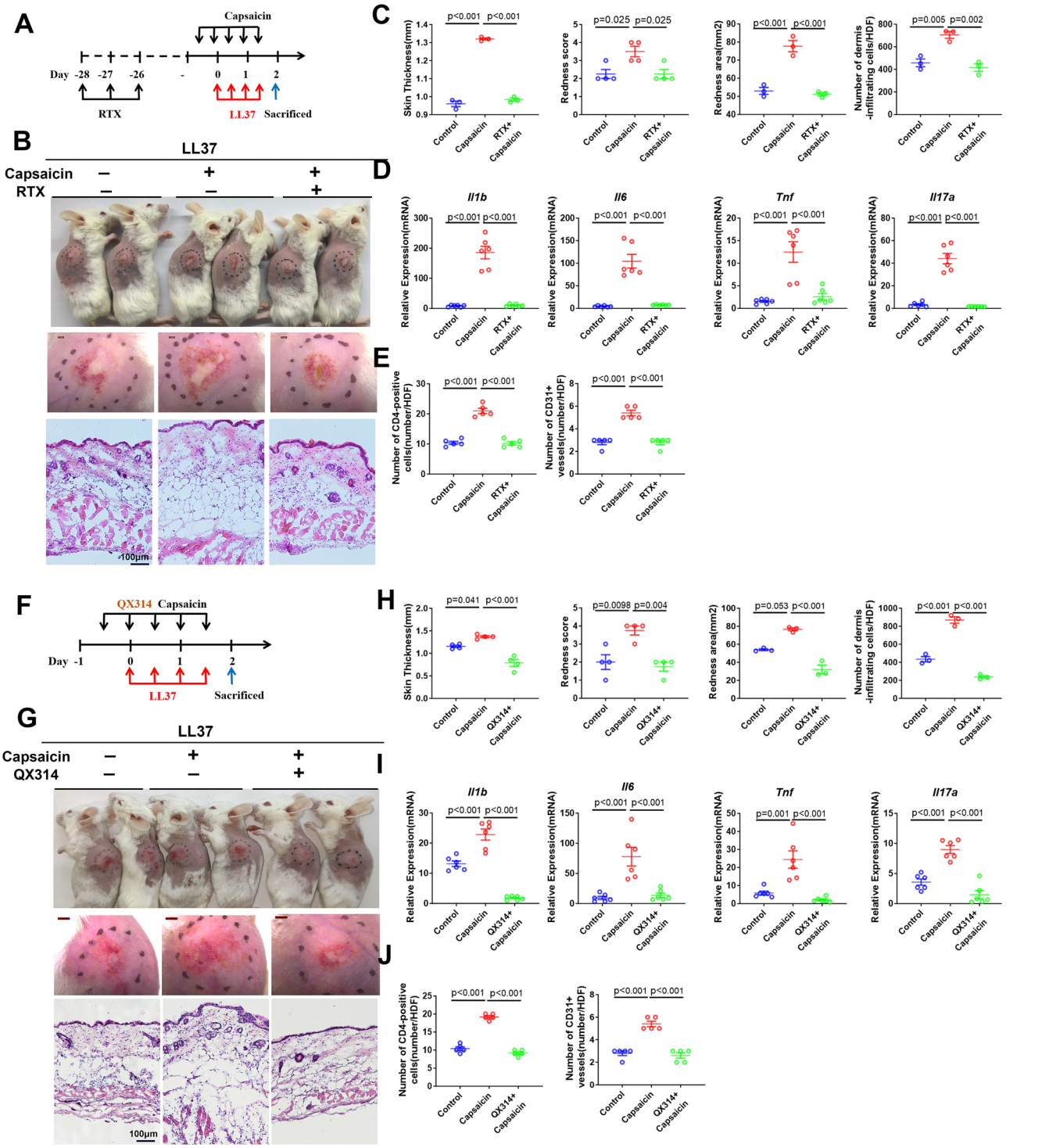

Fig. 2 | Pharmacological ablation of nociceptors abolishes capsaicin-induced exacerbation of rosacea-like dermatitis. A Diagram of the experimental paradigm in **A**–**E**. Nociceptor ablation and induction of rosacea-like skin inflammation. Mice were treated with DMSO or RTX and rested for 4 weeks and then with capsaicin or vehicle on day -1 before intradermal injection of LL37 in mice. **B** Representative photo and HE staining. **C** Redness score, area of erythema and skin thickness ($n = 3$ or 4 mice for each group). **D** mRNA levels of rosacea-characteristic factors ($n = 6$ for each group). **E** $CD4^+$ T cells infiltration and $CD31^+$ microvasculature in the skin of vehicle- or capsaicin-treated RTX mice after LL37 injection. The quantitative analysis of $CD4^+$ T cells and $CD31^+$ microvasculature from pictures originally magnified ×20 ($n = 5$ for each group). **F** Diagram of the experimental paradigm in (**G**–**J**). Mice were co-administered capsaicin with QX314 (100 μM) on day -1 before intradermal injection of LL37. **G** Representative photo and HE staining and (**H**) The redness score, area of erythema and skin thickness ($n = 3$ or 4 for each group) and (**I**) The mRNA levels of rosacea-characteristic factors ($n = 6$ for each group) and (**J**) The $CD4^+$ T cells infiltration and the $CD31^+$ microvascular in the skin of vehicle or capsaicin-treated QX314 mice after LL37 injection ($n = 5$ for each group). **C**–**E** and **H**–**J** Data represent the mean ± SEM. ns, $p > 0.05$. Two-way ANOVA with Bonferroni's post hoc test was used.

https://doi.org/10.1038/s41467-024-50970-1

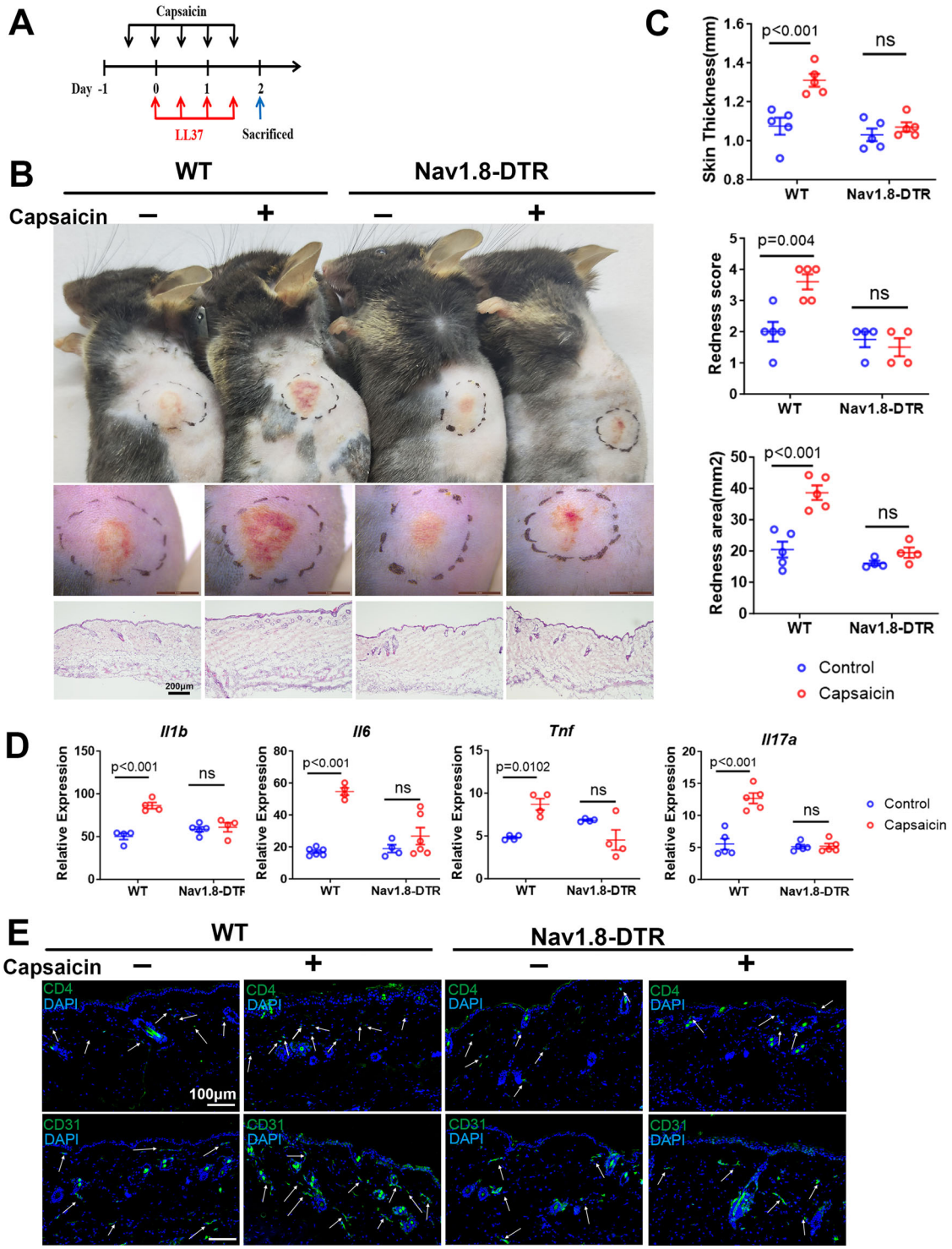

Fig. 3 | Genetic ablation of sensory neurons abolishes capsaicin-inducing exacerbation of rosacea-like dermatitis. A Diagram of the experimental paradigm in (**A**–**E**). Capsaicin or vehicle on day -1 before intradermal injection of PBS or LL37 in WT or Nav1.8-DTR mice. **B** Representative photo and HE staining and (**C**) The redness score, area of erythema and skin thickness ($n = 5$ for each group) and (**D**) The mRNA levels of rosacea-characteristic factors in the skin of vehicle or capsaicin-treated RTX mice after LL37 injection ($n = 4$–6 for each group). Data represent the mean ± SEM. ns, $p > 0.05$. Two-way ANOVA with Bonferroni's post hoc test was used. **E** The $CD4^+$ T cells infiltration and the $CD31^+$ microvascular in the skin of vehicle or capsaicin-treated RTX mice after LL37 injection.

Fig. S9A–E). Subsequently, CGRP was intradermally administered to the mice skin. CGRP treatment alone did not induce skin inflammation, whereas CGRP induced dermatitis aggravation in rosacea-like mice (Fig. 5). In conclusion, these results suggest a requirement for the neuropeptide CGRP, produced by sensory nerves, in capsaicin-mediated dermatitis aggravation.

γδ T cells are essential for the pathogenesis of rosacea-like dermatitis

Next, we sought to identify the target cells regulated by sensory nerves in the skin of rosacea. Previous studies showed that neuropeptides, secreted by nociceptors, can directly signal to immune cells by targeting their receptors[21], and *Ramp1* and *Calcrl* are well-

https://doi.org/10.1038/s41467-024-50970-1

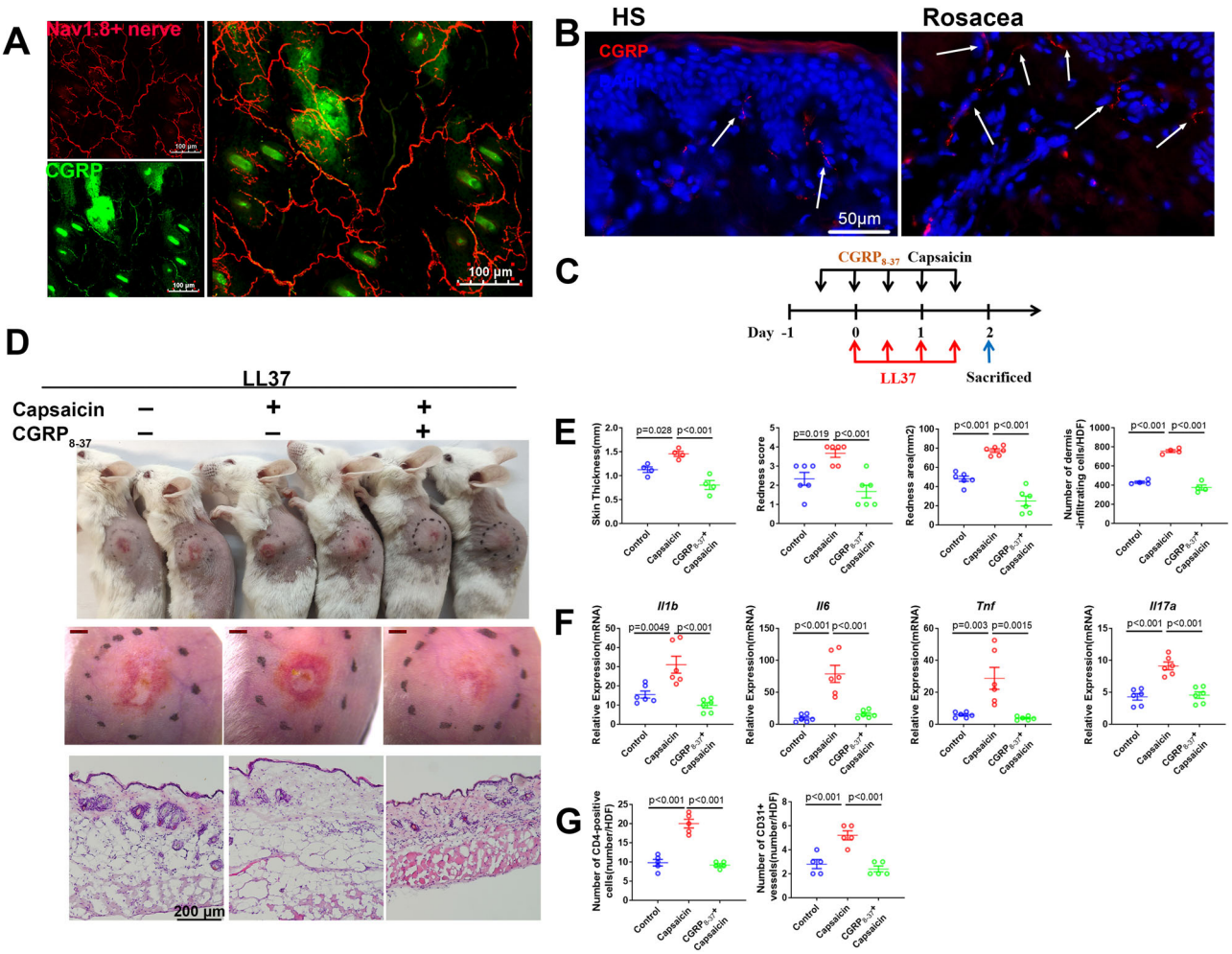

Fig. 4 | CGRP is essential for capsaicin-induced exacerbation of rosacea-like dermatitis. A Representative whole-mount image of capsaicin-treated skin from Nav1.8RFP mice with LL37 injection stained for CGRP. **B** Representative image of CGRP expression in the skin of healthy volunteer (HS) and rosacea patients (Rosacea). **C** Diagram of the experimental paradigm in **(D–G)**. Mice were co-administered capsaicin with $CGRP_{8-37}$ on day −1 before intradermal injection of PBS or LL37. **D** Representative photo and HE staining and (**E**) The redness score, area of erythema and skin thickness of skin tissues ($n = 4$ or 6 for each group) and (**F**) The mRNA levels of rosacea-characteristic factors ($n = 6$ for each group) and (**G**) The $CD4^+$ T cells infiltration and the $CD31^+$ microvascular in the skin of $CGRP_{8-37}$ and capsaicin-treated mice after LL37 injection ($n = 5$ for each group). Data represent the mean ± SEM. ns, $p > 0.05$. Two-way ANOVA with Bonferroni's post hoc test was used.

known receptors of the CGRP neuropeptide. We surveyed immune cells for the expression of *Ramp1* and *Calcrl* using the single-cell transcriptome of skin (Supplementary Fig. S10A). We found that γδ T cells expressed high levels of Ramp1, and the number of γδ T cells was increased in the skin of rosacea patients and rosacea-like mice (Fig. 6A and Supplementary Fig. S10B). We next investigated the role of γδ T cells in rosacea using T-cell receptor delta chain (Tcrd) knockout ($Tcrd^{-/-}$) mice. As shown in Fig. 6B, C, γδ T-cell loss-of-function mice demonstrated thinner skin and weaker erythema than WT mice after LL37 treatment injection. Significant histological change was observed in the skin of γδ T cell loss-of-function mice under LL37 treatment (Fig. 6B, C). Moreover, the increased $CD31^+$ vessels and immune cell infiltration, including $CD4^+$ cells, macrophages, and neutrophils, were evidently abolished in $Tcrd^{-/-}$ mice (Fig. 6D–F and Supplementary Fig. S11). These results indicated that γδ T cells are increased in rosacea and essential for LL37-induced rosacea-like dermatitis.

CGRP-dependent rosacea-like disease is dependent on γδ T cells

Immune cells reside in close proximity to nerves and are rapidly and directly activated/inhibited by neuron-released neuropeptides locally in the skin. Remarkably, immunofluorescence and whole mounts revealed that γδ T cells were in close proximity to sensory nerves both in the skin of human and mouse (Supplementary Fig. S12A and B, and Supplementary Movie 1). Moreover, more γδ T cells were activated and recruited in dermatitis after capsaicin stimulation, which was rescued by QX314 and RTX-mediated nerve ablation (Supplementary Fig. S12C). Consistently, $CGRP_{8-37}$ treatment rescued the increased γδ T cells by capsaicin stimulation, and CGRP treatment increased γδ T cells in rosacea-like dermatitis (Supplementary Fig. S12C).

Subsequently, γδ T-cell loss-of-function ($Tcrd^{-/-}$) mice were treated with capsaicin to assess the role of γδ T cells in capsaicin-aggregated rosacea-like dermatitis. The capsaicin-induced erythema area and skin thickness were reduced in γδ T-cell loss-of-function mice, which is consistent with the weaker skin inflammation that was observed in these mice (Fig. 7A–E). Moreover, CGRP treatment did not aggravate rosacea-like dermatitis in $Tcrd^{-/-}$ mice (Supplementary Fig. S13A–E).

Previous work showed that DDC-derived IL23 is critical to driving psoriasiform skin inflammation by inducing γδ T cell-mediated IL17F and IL22 secretion[5]. Of note, although IL23A mRNA was

https://doi.org/10.1038/s41467-024-50970-1

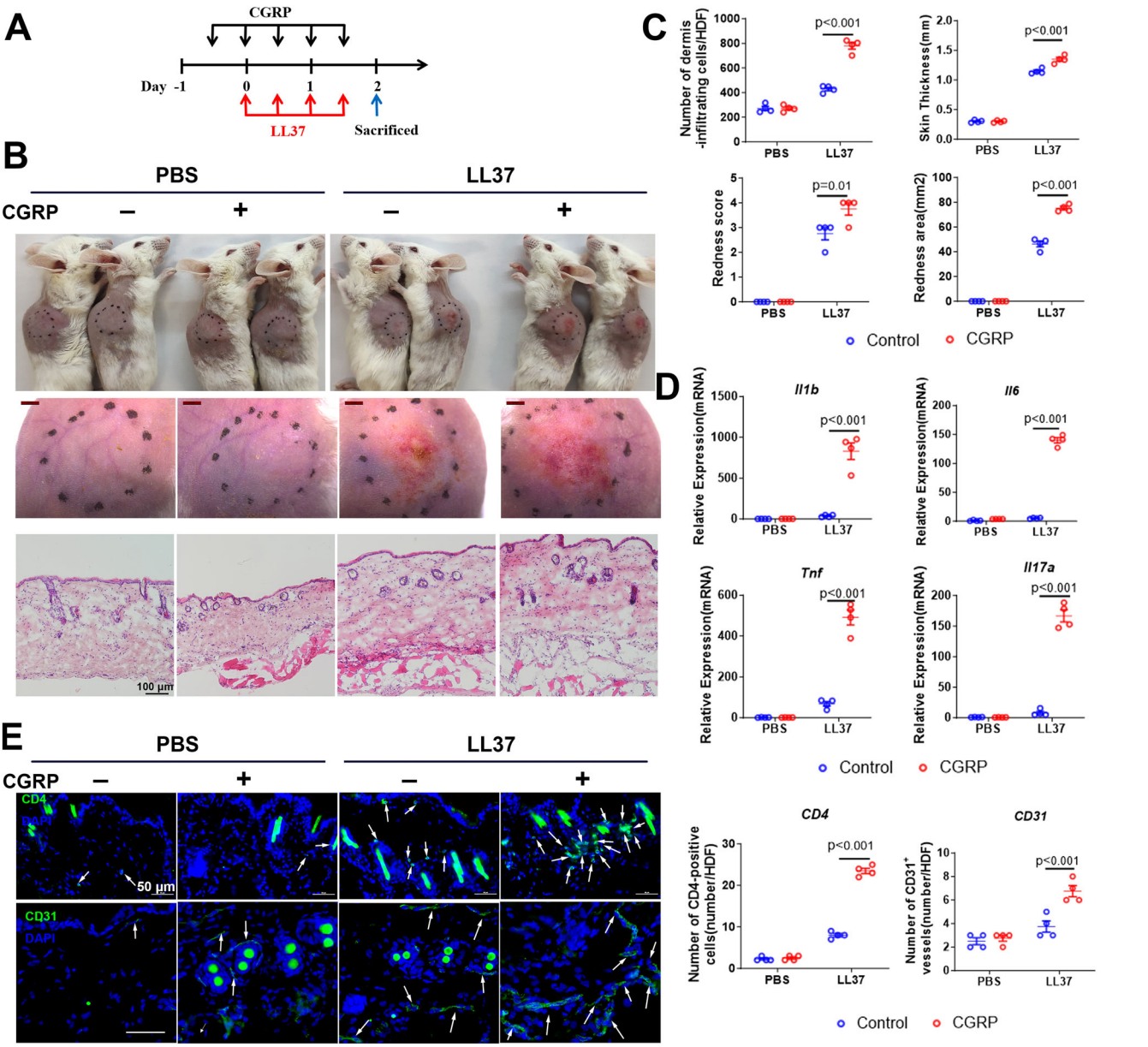

Fig. 5 | CGRP-induced dermatitis aggravation in rosacea-like mice. A Diagram of the experimental paradigm in (**A**–**E**). Mice were treated with CGRP and intradermal injection of PBS or LL37. **B** Representative photo and HE staining and (**C**) The redness score, area of erythema and skin thickness ($n = 4$ for each group) and (**D**) The mRNA levels of rosacea-characteristic factors ($n = 4$ for each group) and **E**, The $CD4^+$ T cells infiltration and the $CD31^+$ microvascular in the skin of vehicle or CGRP-treated mice after LL37 or PBS injection ($n = 4$ for each group). **C**–**E** Data represent the mean ± SEM. ns, $p > 0.05$. Two-way ANOVA with Bonferroni's post hoc test was used.

upregulated in LL37-induced rosacea-like skin, no significant change was observed in the skin lesions of rosacea patients (Supplementary Fig. S14A, our previous transcriptome data HRA000378). Moreover, IL23 knockdown did not affect LL37-induced rosacea-like dermatitis or capsaicin-mediated aggregation in $IL23^{-/-}$ mice (Supplementary Fig. S14B–F).

γδ T cells are involved in inflammation by secreting IFNγ and IL17. Therefore, we assessed the expression of IFNγ and IL17 in rosacea-like mice. Flow cytometry results showed that $IL17A^+$ immune cells were significantly increased in rosacea-like mice (Fig. 8A). IL17A expression was significantly reduced in γδ T cell loss-of-function mice, whereas IFNγ was unaffected (Fig. 6D and Supplementary Fig. S15). The decreased $IL17A^+$ immune cells were also obsereved in $Tcrd^{-/-}$ mice (Fig. 8B). Subsequently, we sorted γδ T cells from the spleen and then stimulated γδ T cells with CGRP. As shown in Fig. 8C, CGRP treatment activated γδ T cells with increased the expression of R*ora* and *Il17a*. Moreover, CGRP treatment also increased IL17A secretion (Fig. 8C and D). Furthermore, the proteomic analysis of γδ T cells was performed to further elucidate the potential mechanism by which CGRP activates γδ T cells. A total of 4212 proteins were detected in γδ T cells by LC–MS/MS, and PCA analysis showed that CGRP treatment significantly affected the protein expression of γδ T cells (Supplementary Fig. S16 A). The GSVA analysis showed that metabolism- and inflammation-related pathways were dysregulated in γδ T cells after CGRP treatment, including GLYCOLYSIS_AND_GLUCONEOGENESIS, INTERLEUKIN_17_SIGNALING, RESPONSE_TO_CHEMOKINE, and POSITIVE REGULATION_OF_MAST_CELL_ACTIVATION (Fig. 8E). A total of 859 differentially expressed proteins (DEPs) were identified with $|\log FC| > 0.5$ and $p < 0.05$ (Fig. 8F and Supplementary Fig. S16B). These DEPs were enriched in metabolism pathways, including cholesterol metabolism,

https://doi.org/10.1038/s41467-024-50970-1

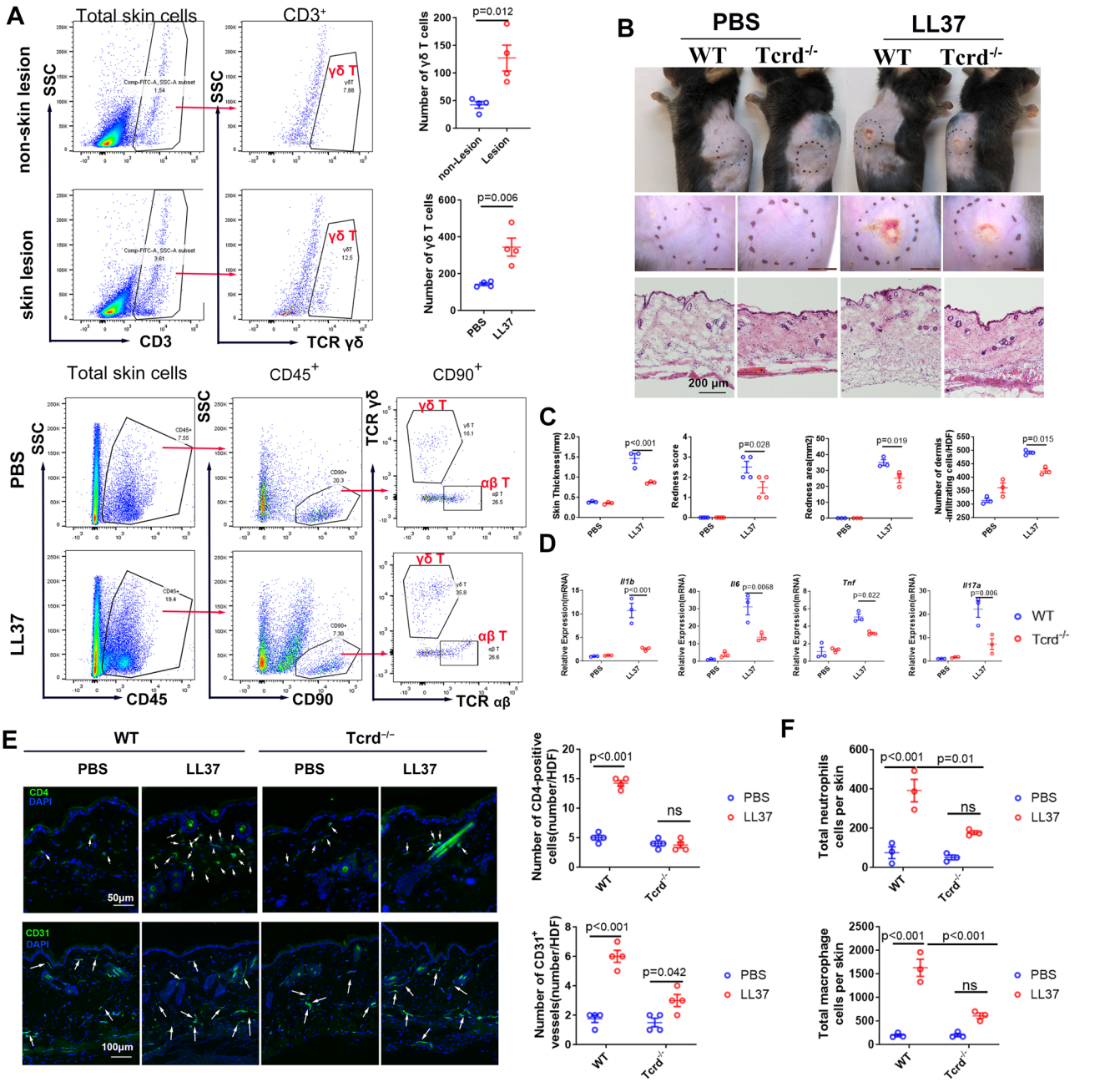

Fig. 6 | γδ T-cell infiltration is increased and essential for the pathogenesis of rosacea. A Representative FACS plots and quantification of γδ T cells in the skin from rosacea patients and rosacea-like mice ($n = 4$ for each group). **B** Representative macroscopic images and HE-stained sections and (**C**) The redness score, area of erythema and skin thickness of skin tissues in WT or Tcrd$^{-/-}$ mice with LL37 or PBS injection ($n = 3$–4 for each group). **D** The mRNA levels of rosacea-characteristic factors ($n = 3$ for each group) and (**E**) CD4$^+$ T cells infiltration ($n = 4$ for each group) and CD31$^+$ microvasculature ($n = 5$ for each group) in the skin of WT or Tcrd$^{-/-}$ mice injected with LL37 or PBS. **F** The quantification of immune cells in the skin from rosacea-like mice ($n = 3$ for each group). Data represent the mean ± SEM. ns, $p > 0.05$. Two-way ANOVA with Bonferroni's post hoc test was used.

glycolysis/gluconeogenesis, fatty acid biosynthesis, the AMPK signaling pathway, the Notch signaling pathway, and the mTOR signaling pathway. Moreover, some DEPs were related to inflammatory signals, including STAT1 signaling, PI3K-AKT signaling and IL17 signaling (Fig. 8G and Supplementary Fig. S16C). Consistent with our proteome results, these metabolism- and inflammation-related pathways are involved in γδ T-cell activity[22–27].

In conclusion, these results indicate that γδ T cells surround sensory nerve endings, and stimulations activate nerves to secrete CGRP, which further induces the accumulation and activation of γδ T cells, thereby aggravating skin inflammation in rosacea-like mice.

Rimegepant attenuated nerve-mediated aggravation of rosacea-like dermatitis

Given the important role of CGRP we found in rosacea, we speculated that it is an effective target for rosacea. Rimegepant is a CGRP receptor antagonist that has shown efficacy and safety in the acute treatment of migraine[28]. We investigated the therapeutic effect of rimegepant on rosacea-like dermatitis. Consistent with the role of $CGRP_{8\text{-}37}$ in this model, rimegepant decreased erythema and skin thickness, which is consistent with the weaker skin inflammation that was observed in these mice (Fig. 9A–E). Rimegepant did not affect ATF3 expression in the DRG of rosacea-like mice (Supplementary Fig. S17A), whereas the capsaicin-induced increase in γδ T cells was significantly rescued by

https://doi.org/10.1038/s41467-024-50970-1

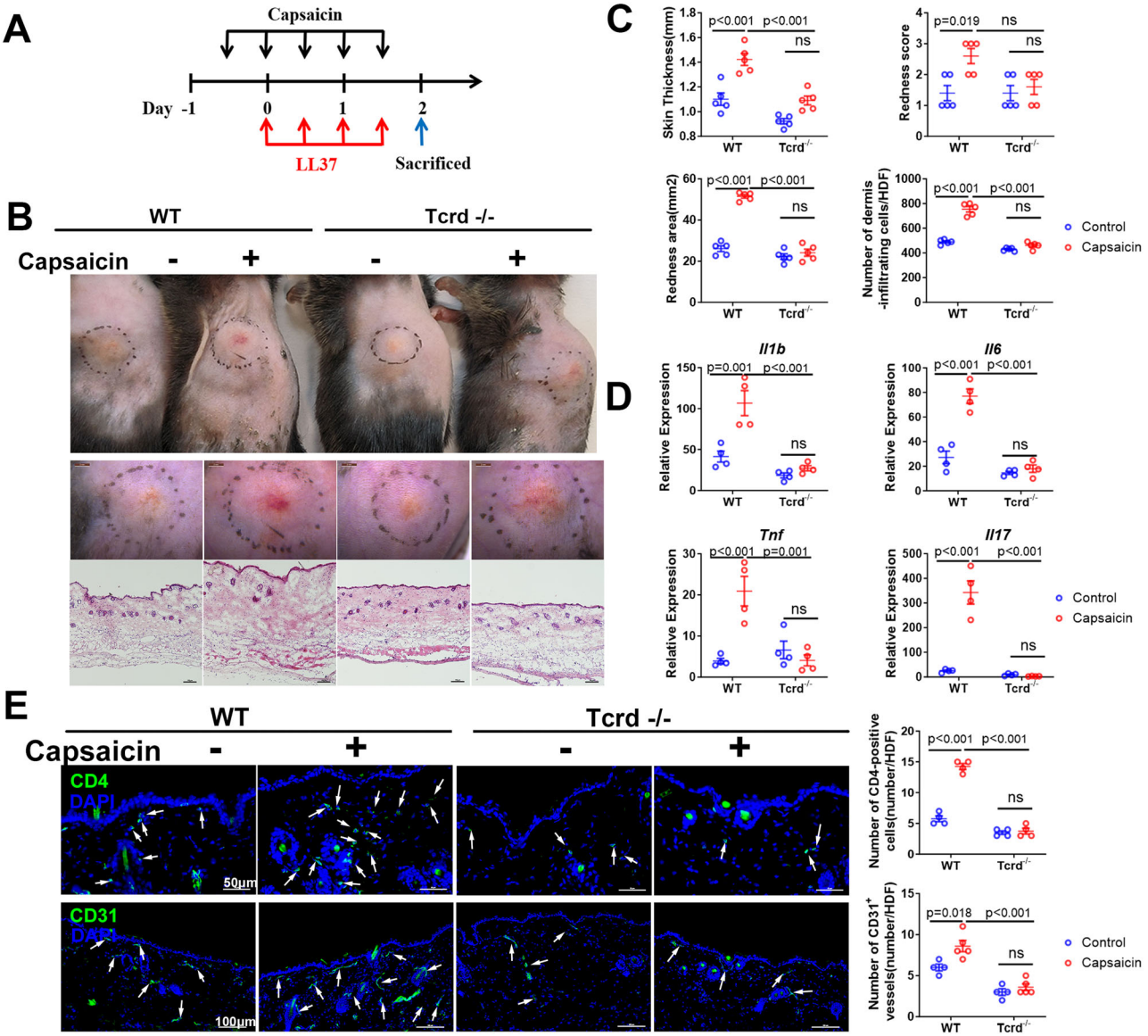

Fig. 7 | Sensory nerve-secreted CGRP activates γδ T cells directly. A Diagram of the experimental paradigm in (**A**–**E**). Capsaicin or vehicle on day −1 before intradermal injection of LL37 in WT or Tcrd$^{-/-}$ mice. **B** Representative macroscopic images and HE-stained sections and **C** The redness score, area of erythema and skin thickness of skin tissues in vehicle or capsaicin-treated WT or Tcrd$^{-/-}$ mice after LL37 injection ($n = 5$ mice for each group). **D** The mRNA levels of rosacea-characteristic factors and **E** CD4$^+$ T cells infiltration and CD31$^+$ microvasculature in the skin of vehicle- or capsaicin-treated WT or Tcrd$^{-/-}$ mice after LL37 injection ($n = 4$ for each group). **C**–**E** Data represent the mean ± SEM. ns, $p > 0.05$. Two-way ANOVA with Bonferroni's post hoc test was used.

rimegepant treatment in rosacea-like mice (Supplementary Fig. S17B). These data suggest that rimegepant could be an effective treatment for hypersensitive nerve-mediated aggravation of rosacea-like dermatitis.

Discussion

Rosacea is characterized by immune disturbances that are triggered and aggravated by chemical (capsaicin) or thermal (heat/cold) stimuli. Here, we demonstrate that capsaicin activates nociceptors to aggravate rosacea-like dermatitis by releasing CGRP. Mechanistically, γδ T cells are essential for rosacea-like dermatitis, and they are closely associated with cutaneous nerves and can be directly activated by CGRP.

The skin is densely innervated by sensory fibers, most of which express markers of nociceptors, including TRPV1 and Nav1.8 channels. They cooperate with immune cells and are involved in the pathogenesis of various skin disorders[5–7]. Stimulus factors (such as heat and capsaicin) trigger and aggravate rosacea, indicating the important role of sensory nerve. Activated neurons were observed in the DRG of rosacea-like mice, consistent with previous studies that inflammation in the skin can induce the activation of neurons[29]. However, our previous work[19] and this work (Supplementary Fig. S1) showed that sensory nerves and sympathetic nerves ablation did not influence rosacea-like dermatitis. As previously described[19], neuron activation is insufficient to influence skin inflammation in two-days rosacea-like dermatitis.

Considering the facial hyperresponsiveness of rosacea patients to stimulus factors, we treated rosacea-like mice with capsaicin to simulate hypersensitive rosacea skin, in order to explore the neuro-immune mechanism in rosacea. Capsaicin, a classical sensory nerve antagonist, is a common trigger that contributes to the pathogenesis of rosacea. Here, we found that capsaicin stimulation did not induce skin inflammation but aggravated rosacea-like dermatitis. Moreover, heat stimulation, another sensory nerve activator, also aggravated rosacea-like

https://doi.org/10.1038/s41467-024-50970-1

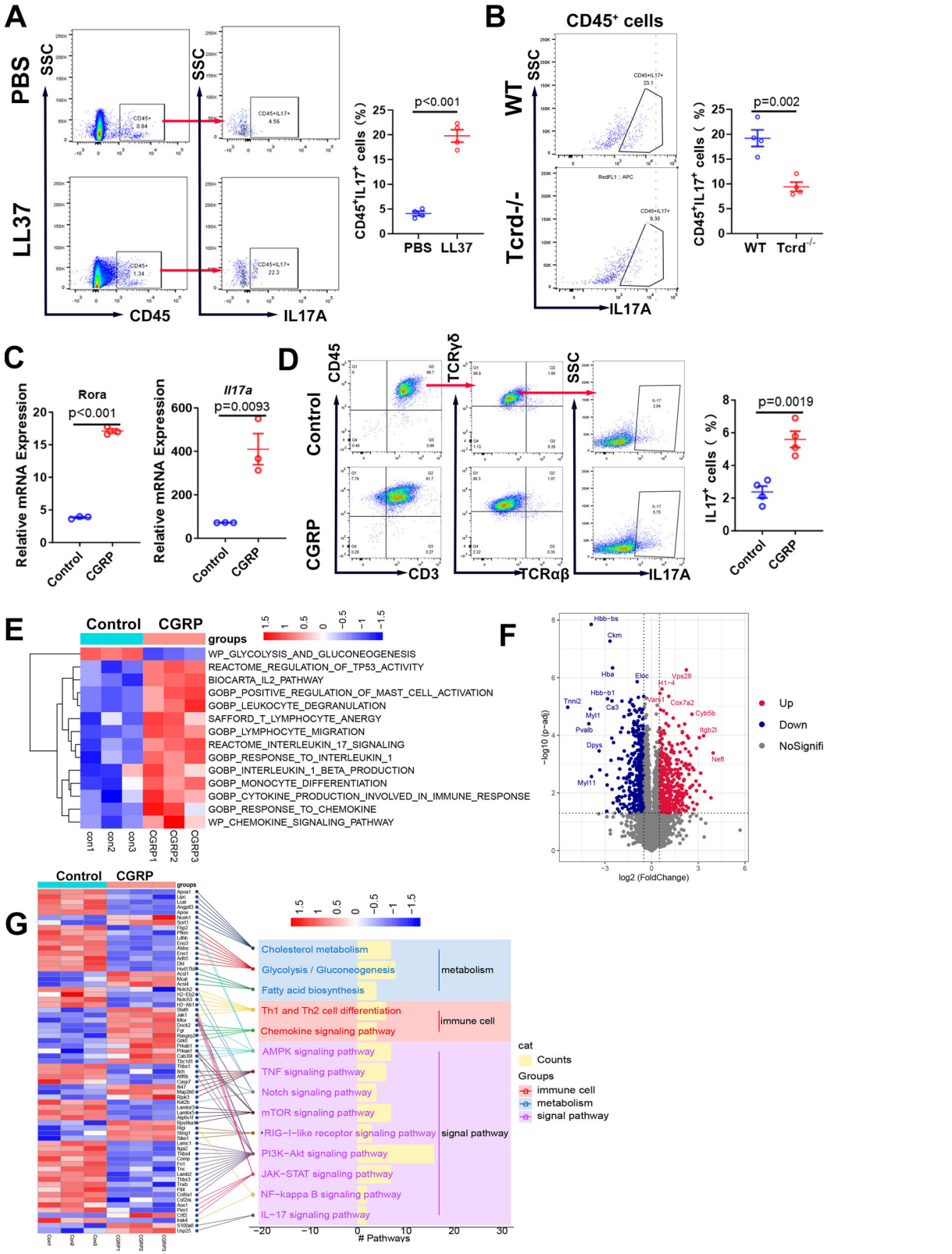

Fig. 8 | CGRP induced γδ T-cell activation. A Flow cytometry of IL17A$^+$ immune cells in rosacea-like skin ($n = 3$ for each group). **B** Flow cytometry of IL17A$^+$ immune cells in the skin of γδ T-cell loss-of-function mice with LL37 injection ($n = 3$ for each group). **C** The IL17A and RORA mRNA levels in γδ T cells after CGRP treatment ($n = 3$ for each group). **D** Flow cytometry revealed IL17A secretin in γδ T cells after CGRP treatment ($n = 4$ for each group). **E** GSVA analysis of the proteins in γδ T cells treated with vehicle or CGRP. **F** Volcano plot of DEPs determined between control and CGRP-treated γδ T cells. **G** Enrichment analysis of DEPs determined between control and CGRP-treated γδ T cells. Data represent the mean ± SEM. ns, $p > 0.05$. Two-way ANOVA with Bonferroni's post hoc test was used.

https://doi.org/10.1038/s41467-024-50970-1

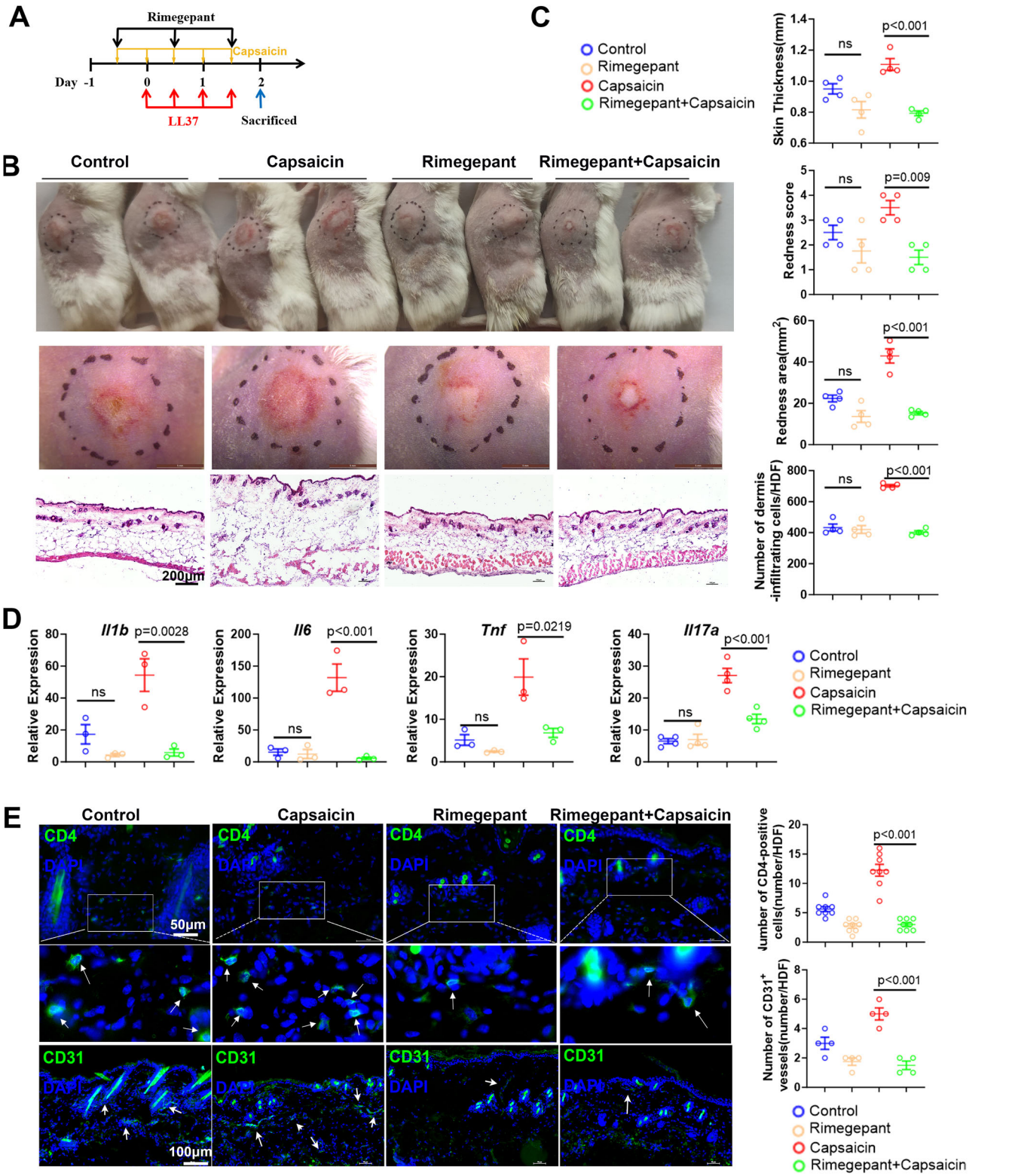

Fig. 9 | Rimegepant attenuated nerve-mediated rosacea aggravation. **A** Diagram of the experimental paradigm in (**A**–**E**). Mice were coadministered capsaicin with rimegepant on day −1 before intradermal injection of PBS or LL37. **B** Representative photo and HE staining and (**C**) The redness score, area of erythema and skin thickness of skin tissues in rimegepant and capsaicin-treated mice after LL37 injection ($n = 4$ for each group). **D** The mRNA levels of rosacea-characteristic factors ($n = 3$ or 4 for each group) and (**E**) $CD4^+$ T cells infiltration ($n = 8$ for each group) and $CD31^+$ microvasculature ($n = 4$ for each group) in the skin of rimegepant and capsaicin-treated mice after LL37 injection. Data represent the mean ± SEM. ns, $p > 0.05$. Two-way ANOVA test was used.

dermatitis but did not induce skin inflammation in normal skin (Supplementary Fig. S18). These results indicated that the nerve is hypersensitive in rosacea-like mice, consistent with the facial hypersensitivity of rosacea patients. Considering the slight activation of the sensory nerve in the DRG of rosacea-like mice, we speculated that the inflammatory microenvironment may partly contribute to the hypersensitivity of nerves. Although increased nerve innervation was not observed in rosacea-like mice, our recent proteome data revealed the increased nerve-related proteins in skin lesions from rosacea patients, implying a potential increase of nerve innervation[30]. Based on these findings, further studies will also be needed to determine whether increased nerve innervation contributes to hyperresponsiveness to the stimulus factor of rosacea.

Nociceptor-derived neuropeptides (such as CGRP, SP), released by activated neurons, can modulate inflammation directly. CGRP is a well-known major neuropeptide secreted by nociceptive sensory nerves, playing a critical role in against infection[31,32], allergic response[33,34], inflammation response[35] and in maintaining barrier homeostasis[21]. During neuroimmune regulation, it is essential for the in direct or close proximity contact between nerves and immune cells[5]. Here, we demonstrated that CGRP is required for nerve-induced dermatitis aggravation in rosacea by activating γδ T cells directly. Notably, although CGRP was reported to drive the DCs/ IL23 response in psoriasiform inflammation[5,11], our study reveals that IL23 knockout did not affect rosacea-like dermatitis or capsaicin-induced aggravation. Previous studies revealed the key role of mast cells in cathelicidin-initiated skin inflammation in rosacea[36]. Nonpeptidergic neurons were reported to maintain skin homeostasis by suppressing mast cells[9]. The sensory neuron-mast cell interactions in the skin have also been reported[37]. These indicated that mast cells may involve in sensory nerve-aggravated rosacea dermatitis, however, this speculation needs to be further clarified.

The type 17 inflammatory response can be elicited by cutaneous sensory nerve activation[17]. Dermal γδ T cells are the major IL17–producing lymphocyte subset within the skin both at steady state and during various infections and inflammatory diseases[15]. Although increased IL17 expression was observed in rosacea[18], the cell types that express IL17 remain unclear. Our findings highlight an additional role of IL17–producing γδ T cells in rosacea pathogenesis and the requirement of this cell in stimulation-driven exacerbated dermatitis upon nociceptor activation. Although CGRP has been reported to activate/inhibit immune cells directly, the specific molecular mechanism has rarely been reported. Ramp1 and Calcrl are well-known CGRP receptors that were recently reported to be expressed in macrophages, involving in immune phenotypic polarization and suppressing chemokine production[38]. We found that γδ T cells highly express Ramp1, the receptor of CGRP. Upon CGRP stimulation, the expression and secretion of IL17A were increased in γδT cells. γδ T cells exert potent cytotoxic effects against infections by producing IFNγ[39]. Although previous studies demonstrated the upregulation of IFNγ and interferon signaling in rosacea[18], we found that IFNγ is not produced by γδ T cells in rosacea. Alessio et al. demonstrated that dysbiotic commensal bacteria drove the type I IFNs produced by plasmacytoid DCs in rosacea[40].

The mechanism of γδ T cell activation was widely studied for several years. Studies have shown that STAT1 signaling[22,23] and PI3K-Akt signaling[24] induce IL17A secretion by γδ T cells. Consistently, these signaling pathways were elevated in γδ T cells after CGRP treatment, implying that CGRP induces γδ T-cell IL17A production partly by activating STAT1 and PI3K-Akt signaling. Although CGRP treatment regulated the metabolism pathways in γδ T cells, recent studies showed that cholesterol metabolism, fatty acid metabolism and glucose metabolism impact the tissue residency and function of γδ T[25–27] by affecting lytic granule but not IL17 secretion[27]. Metabolism-related pathways, including the AMPK pathway[27] and mTOR pathway[41] contribute to the antitumor activity of γδ T cells. Therefore, the underlying mechanism of CGRP regulated inflammation and metabolism in γδ T cells remains to be further clarified.

In summary, we demonstrate the central role of dermal γδ T cells in the pathogenesis of rosacea. Upon stimulation (capsaicin/heat), sensory nerve was activated and secreted CGRP, subsequently activating dermal γδT cells directly, thereby resulting in exacerbated disease severity. These results reveal a nerve/CGRP/γδT cell axis,and could lead to new therapeutic perspectives for rosacea.

Methods

Ethical statement

This study was approved by the ethical committee of the Xiangya Hospital of Central South University (IRB number 201703212). Informed consent was obtained from all participants. IRB approval status: Study further reviewed and approved by xiangya hospital (201404361). Patient consent is on file.

Human skin tissue samples

For rosacea, human skin tissues were collected from the central face region of patients with rosacea (n = 8) and age-matched healthy volunteers (n = 8) (Table S1). All human skin tissues were collected from the Department of Dermatology in Xiangya Hospital, Central South University. The transcriptome data of rosacea (HRA000378) were downloaded from our previous work[42].

Mice

All animal experiments were approved by the Ethics Committee of Xiangya Hospital of Central South University. Mice were housed in a pathogen-free animal facility at Central South University. All mouse experiments were repeated three times, and 5–8 mice were included in each group.

C57BL/6 and BALB/C mice were purchased from SLAC LABORATORY ANIMAL CO. B6.129-Trpv1tm1(cre)Bbm/J, The Tcrd −/− mice were kindly gifted by Professor Zhinan Yin (Zhuhai Institute of Translational Medicine, Jinan University), IL-23p19-/- was kindly gifted by Professor Quanming Zou (Third Military Medical University), DTR-flox was kindly gifted by Professor Jing Feng (Shanghai Institute of Materia Medica, Chinese Academy of Sciences), and Nav1.8-cre mice were kindly gifted by Professor Xiaoyang Cheng. Nav1.8-DTR mice were bred with Nav1.8-cre mice to generate DTR-flox mice. Age-matched 4 to 10-week-old mice were used for experiments. The mice were housed in an environmentally controlled room at 22 ± 2.0 °C and 50% ± 5% humidity, with a 12-h light/dark cycle, and were fed standard rodent chow and tap water. All animal experiments were conducted in a blinded manner.

LL37-induced rosacea-like mouse model

The antimicrobial peptide LL37 was synthesized by Sangon Biotech, and the purity of LL37 was 95% by high performance liquid chromatography (HPLC).

Eight-week-old mice were selected for the experiment. The hair was shaved one day before LL37 injection. A rosacea-like mouse model was constructed by intradermal injection of LL37 peptide as previously described[19]. Rosacea-like dermatitis was assessed based on the severity of erythema and edema. The area of erythema was determined by measurement with a stereomicroscope (Leica S8AP0, Leica, Germany), and the severity of edema was determined by measuring the skin thickness at the erythema site with a Vernier caliper.

Capsaicin was purchased from Sigma Chemical Company (St. Louis, MO). Capsaicin is dissolved in 1.5% sodium vitrate gel prior to each use.

Sensory nerve ablation

RTX treatments: Resiniferatoxin (RTX) a TRPV1 ligand reported to rapidly desensitize TRPV1 receptors, was purchased from Sigma

Table 1 | The primer sequences for RT-qPCR

Primer	Species	Forward(5'to3')	Reverse(5'to3')
GAPDH	mouse	AGGTCGGTGTGAACGGATTTG	TGTAGACCATGTAGTTGAGGTCA
TNF	mouse	CTGAACTTCGGGGTGATCGG	GGCTTGTCACTCGAATTTTGAGA
VEGF	mouse	TATTCAGCGGACTCACCAGC	AACCAACCTCCTCAAACCGT
IL17	mouse	TTTAACTCCCTTGGCGCAAAA	CTTTCCCTCCGCATTGACAC
IL1β	mouse	GCAACTGTTCCTGAACTCAACT	ATCTTTTGGGGTCCGTCAACT
IFN-γ	mouse	GCCACGGCACAGTCATTGA	TGCTGATGGCCTGATTGTCTT
IL6	mouse	TAGTCCTTCCTACCCCAATTTCC	TTGGTCCTTAGCCACTCCTTC
VIP	mouse	AGTGTGCTGTTCTCTCAGTCG	GCCATTTTCTGCTAAGGGATTCT
SP	mouse	AAGCGGGATGCTGATTCCTC	TCTTTCGTAGTTCTGCATTGCG
PACAP	mouse	ACCATGTGTAGCGGAGCAAG	CCTCGTCTTCTGGTCTGATCC
CGRP	mouse	CAGTGCCTTTGAGGTCAATCT	CCAGCAGGCGAACTTCTTCTT
NPY	mouse	ATGCTAGGTAACAAGCGAATGG	TGTCGCAGAGCGGAGTAGTAT
NMU	mouse	GAGGGAGCTTTGCCGTATAGT	GATGCACAACAGAGGACACAA
ATF3	mouse	GAGGATTTTGCTAACCTGACACC	TTGACGGTAACTGACTCCAGC
TAFA4	mouse	CCTATGTGTTAATGGTCTGCTGT	CCACCACTTCTCAATCACAATGG

Chemical Company (St. Louis, MO). RTX was injected subcutaneously into the lateral abdomen of 4-week-old mice at 30/70/100 μg/kg on three consecutive days, and after a successful tail-flick assay, the LL37-induced rosacea-like dermatitis was established 4 weeks after the last RTX injection.

QX314 treatments: QX314 chloride is a membrane-impermeable permanent charge blocker of sodium channels that was purchased from Sigma Chemical Company (St. Louis, MO). One day before constructing rosacea-like dermatitis, QX314 was injected intradermally into the back of the mice at 100 μM per dose, followed by simultaneous injection of QX314 with each injection of LL37.

Diphtheria Toxin Depletion: Nav1.8-DTR mice were injected intraperitoneally (i.p.) with 100 ng of DT (Sigma-Aldrich) for 3 consecutive days.

$CGRP_{8-37}$ treatments: $CGRP_{8-37}$ is a CGRP receptor antagonist. The rosacea-like dermatitis was constructed by intradermal injection of $CGRP_{8-37}$ (Genescript) into the backs of mice one day before construction, and then $CGRP_{8-37}$ was injected at the same time as each LL37 injection.

CGRP treatments: Mice were injected intradermally with CGRP (Genescript) each time on the dorsal side of the back one day before rosacea modeling, and the same dose of CGRP was injected at the same time as each subsequent injection of LL37.

Rimegepant treatments: Rimegepant is a CGRP receptor antagonist. One day before the subcutaneous injection of LL37, mice were gavaged with 0.2 mg once a day for three days. Afterwards, LL37 was injected intradermally to construct a rosacea-like model.

Histological analysis

Skin samples were fixed in formalin and then embedded in paraffin. Tissue sections were cut into 4 μm thick sections and stained with hematoxylin and eosin (HE). The number of infiltrating cells in the dermis was counted.

RT-qPCR

Total RNA was extracted from mouse skin tissues, DRG, and cells using TRIzol reagent. mRNA was reverse-transcribed using the Maxima H Minus First Strand cDNA Synthesis Kit with dsDNase (K1682, Thermo Fisher) according to the manufacturer's instructions. qPCR was performed on a LightCycler 96 (Roche) thermal cycler using the iTaq™ Universal SYBR® Green Supermix (Bio-Rad). The relative expression of each gene relative to the internal control gene GAPDH was calculated by the ΔCT method. Fold changes for each gene were normalized to the control. The primer sequences specific to each gene are in Table 1.

Immunofluorescence

Skin and DRG (dorsal root ganglion) were embedded using OCT and cut into frozen sections with a thickness of 8 μm. The frozen sections were fixed with 10% PFA for 10 min, then washed three times with PBS and closed with containment buffer (95% PBS, 5% NDS, 0.3% Triton X-100) for 60 min. The indicated primary antibodies were incubated overnight at 4 °C. The next day, PBS was washed three times, followed by incubation with Alexa Fluor 594-coupled secondary antibody (1:500, ThermoFisher) for 60 min at room temperature. After washing with PBS, staining was done with DAPI (1:2000). All images were taken using a Zeiss Axioplan 2 microscope. The following primary antibodies were used: Anti-Mouse CD4 (1:200, eBioscience, 14-0042-85), Anti-Mouse CD31 (1:200, BD Biosciences, 558736), anti-CGRP (1:200, Cell Signaling Technology, 14959), anti-CGRP (1:200, Abcam, ab36001), hamster anti-γδT (1:200, Biolegend, 118101), anti-human-γδT (1:200, Biolegend, 331235), and rabbit anti-ATF3 (1:200, Abcam, ab254268), anti-RFP (1:200, Rockland, 600-401-379).

Extraction and culture of γδ T cells

The γδ T cells sorting was performed using the TCRγ/δ + T Cell Isolation Kit (Miltenyi Biotec, 130-092–125). Mouse spleens and lymph nodes were collected and grinded to form a suspension of cells. Then erythrocyte lysate was added to lysed erythrocytes. Non-T cells were labeled by Non-T Cell Depletion Cocktail of MicroBeads and γδ T cells were sorted in MACS Separator by MS Column. The collected cells were inoculated with the density of 10^6/ml. The purity of the cells was determined by flow cytometry. The CGRP-treated group was incubated with 0.4 μg/ml of CGRP for 12 h.

LC-MS/MS mass spectrometry-based proteomics

Sorted γδ T was ground in 100 μl of lysis solution and the protein was obtained by centrifuging at 12000 × *g* for 20 minutes. After quantification of protein concentration by bicinchoninic acid assay (Thermo Fisher Scientific, USA), 20 μg protein samples were processed according to the kit instructions (Omicsolution, China). The peptides were then separated by a Thermo NanoVipe-C18 column (25 cm × 75 mm) using a Vanquish Neo HPLC system (Thermo Fisher Scientific, USA) and analyzed using an Orbitrap Exploris 480 mass spectrometer (Thermo Fisher Scientific, USA). DIA raw data was analyzed using Spectronaut (v 18).

Proteomics analysis

The limma R package was used for differentially expressed analysis between the control and CGRP group, and proteins with an adjusted

p-value < 0.05 and |log2(FoldChange)|>=0.5 were considered as differentially expressed proteins (DEPs). GO and KEGG enrichment analysis of the DEPs were performed using the clusterProfiler R package, and an adjusted p-value of 0.05 was set as the threshold for significance. The GSVA analysis was used for estimating the activation of pathways using R packages "GSVA" and "GSEABase". The different pathways and DEPs were shown in the heatmap using R package "pheatmap".

Flow cytometry

Skin tissues from mice and human (skin lesion and non-lesion from 4 rosacea patients) were minced and incubated in DMEM medium containing Collagenase IV (2 mg/ml) + dispase II (1 mg/ml) (*Worthington* Biochemical). at 37 °C for 100 min. Digestion was stopped with DMEM containing 10% fetal bovine serum and filtered through a 70 μm cell filter. Cells were reselected using a culture medium containing PMA 50 ng/ml + ionomycin 500 μg/ml + Monensin (1:1500) and incubated at 37 °C for 5 h. After washing, the cells were pre-incubated with Zombie Aqua™ dye or Fixable Viability Stain 510 (564406, BD Pharmingen, CA, USA) and Fc Block (101320) and then were stained for surface antigens 30 min at 4 °C in the dark. The antibodies included: FITC anti-mouse CD45 (552950, BD Pharmingen, USA), APC-Cy7 anti-mouse CD90.2 (561641, BD Pharmingen, USA), PE-Cy7 anti-mouse TCR Bta Chain (560729, BD Pharmingen, USA), PE anti-mouse TCR γ/δ(560729, BD Pharmingen, USA), PerCP-Cy5.5 anti-mouse CD3 (100218, Biolegend, USA), Pacific Blue anti-mouse CD11b (560455, BD Pharmingen, USA), PE-Cy7 anti-mouse CD11c (558079, BD Pharmingen, USA), PE anti-mouse F4 /80 (565410, BD Pharmingen, USA), Alexa Fluor® 647 anti-I-A/I-E (562367, BD Pharmingen, CA, USA), Alexa647 anti-mouse IL−17A (506912, BD Pharmingen, CA, USA), Fixable Viability Stain 510 (564406, BD Pharmingen, CA, USA), and PerCP-Cy5.5 anti-mouse ly6G (560602, BD Pharmingen, CA, USA), FITC anti-human CD3 Antibody (317306, BD Pharmingen, CA, USA), PE/Cy7 anti-human TCR α/β Antibody (306719, Biolegend, USA), PerCP/Cy5.5 anti-human TCR γ/δ Antibody(331223, Biolegend, CA, USA). Cells were then fixed and permeabilized using the BD Cytofix/Cytoperm kit (BD Pharmingen, CA, USA), and then were incubated with PE anti-mouse IL−17A (506903, Biolegend, USA), Alexa647 anti-mouse IL−17A (506912, Biolegend, USA), PE anti-human IL−17A Antibody (512305, Biolegend, USA), TruStain fcX™ (anti-mouse CD16/32) (101320).

Whole-mount immunofluorescence

Skin tissues were shaved and fixated in 4% paraformaldehyde, and then tissues were stained with antibodies in a blocking buffer (10% goat serum, 1% Triton X−100). anti-CGRP (1:200, Abcam, ab36001), hamster anti-γδT (1:200, Biolegend, 118101). The images were acquired on Two-Photon Microscopy (Olympus) with the software FV31S-SW (Olympus). Post-acquisition image analysis was performed using Imaris software (Bitplane scientific software).

Statistical analyses

The experimental numbers of animals were described in the figure legends. All experiments were repeated at least three times. Statistical analyses were performed using GraphPad 8.0. Data are shown as the mean ± SEM. Normal distribution and similar variance between groups were analyzed. Differences between the two groups were compared using a two-tailed unpaired Student's t-test. One-way or two-way analysis of variance (ANOVA) with relevant post hoc tests was used for multiple comparisons ($^{*}p < 0.05$, $^{**}p < 0.01$, $^{***}p < 0.001$). The two-tailed Mann−Whitney *U* test was performed for data that were not normally distributed or if the variances of the two groups were unequal.

Reporting summary

Further information on research design is available in the Nature Portfolio Reporting Summary linked to this article.

Data availability

The data and the code that support the findings of this study are available in the article and its Supplementary Files or on request from the corresponding authors. The scRNA data of mice and human skin were downloaded from Gene-Expression Omnibus (GSE150672 and GSE149121). The proteomics data generated in this study have been deposited in the ProteomeXchange Consortium through the iProX partner repository under accession code PXD047082. Other data supporting the findings of the present study are available from the corresponding author (Ji Li, E-mail: liji_xy@csu.edu.cn). Source data are provided in this paper.

References

1. Ezra, N., Greco, J. F., Haley, J. C. & Chiu, M. W. Gnatophyma and otophyma. *J. Cutan. Med. Surg.* **13**, 266–272 (2009).
2. Cribier, B. [Rosacea: new data for better care]. *Ann. Dermatol Venereol.* **144**, 508–517 (2017).
3. Halioua, B., Cribier, B., Frey, M. & Tan, J. Feelings of stigmatization in patients with rosacea. *J. Eur. Acad. Dermatol. Venereology: JEADV* **31**, 163–168 (2017).
4. Wienholtz, N. K. F. et al. Infusion of pituitary adenylate cyclase-activating polypeptide-38 in patients with rosacea induces flushing and facial edema that can be attenuated by sumatriptan. *J. investigative Dermatol.* **141**, 1687–1698 (2021).
5. Riol-Blanco, L. et al. Nociceptive sensory neurons drive interleukin-23-mediated psoriasiform skin inflammation. *Nature* **510**, 157–161 (2014).
6. Yamamoto, Y. et al. Pituitary adenylate cyclase-activating polypeptide promotes cutaneous dendritic cell functions in contact hypersensitivity. *J. allergy Clin. Immunol.* **148**, 858–866 (2021).
7. Filtjens, J. et al. Nociceptive sensory neurons promote CD8 T cell responses to HSV-1 infection. *Nat. Commun.* **12**, 2936 (2021).
8. Hoeffel, G. et al. Sensory neuron-derived TAFA4 promotes macrophage tissue repair functions. *Nature* **594**, 94–99 (2021).
9. Zhang, S. et al. Nonpeptidergic neurons suppress mast cells via glutamate to maintain skin homeostasis. *Cell* **184**, 2151–2166.e2116 (2021).
10. Xu, M. et al. Activation of CD81(+) skin ILC2s by cold-sensing TRPM8(+) neuron-derived signals maintains cutaneous thermal homeostasis. *Sci. Immunol.* **7**, eabe0584 (2022).
11. Kashem, S. W. et al. Nociceptive sensory fibers drive interleukin-23 production from CD301b+ dermal dendritic cells and drive protective cutaneous immunity. *Immunity* **43**, 515–526 (2015).
12. Girardi, M., Lewis, J. M., Filler, R. B., Hayday, A. C. & Tigelaar, R. E. Environmentally responsive and reversible regulation of epidermal barrier function by gammadelta T cells. *J. investigative Dermatol.* **126**, 808–814 (2006).
13. Nielsen, M. M. et al. NKG2D-dependent activation of dendritic epidermal T cells in contact hypersensitivity. *J. investigative Dermatol.* **135**, 1311–1319 (2015).
14. Jee, M. H., Mraz, V., Geisler, C. & Bonefeld, C. M. γδ T cells and inflammatory skin diseases. *Immunological Rev.* **298**, 61–73 (2020).
15. Sandrock, I. et al. Genetic models reveal origin, persistence and non-redundant functions of IL-17-producing γδ T cells. *J. Exp. Med.* **215**, 3006–3018 (2018).
16. Cai, Y. et al. Pivotal role of dermal IL-17-producing γδ T cells in skin inflammation. *Immunity* **35**, 596–610 (2011).
17. Cohen, J. A. et al. Cutaneous TRPV1(+) neurons trigger protective innate type 17 anticipatory immunity. *Cell* **178**, 919–932 (2019).
18. Buhl, T. et al. Molecular and morphological characterization of inflammatory infiltrate in rosacea reveals activation of Th1/Th17 pathways. *J. investigative Dermatol.* **135**, 2198–2208 (2015).

19. Zhang, Y. et al. Nav1.8 in keratinocytes contributes to ROS-mediated inflammation in inflammatory skin diseases. *Redox Biol.* **55**, 102427 (2022).
20. Braz, J. M. & Basbaum, A. I. Differential ATF3 expression in dorsal root ganglion neurons reveals the profile of primary afferents engaged by diverse noxious chemical stimuli. *Pain* **150**, 290–301 (2010).
21. Yang, D. et al. Nociceptor neurons direct goblet cells via a CGRP-RAMP1 axis to drive mucus production and gut barrier protection. *Cell* **185**, 4190–4205.e4125 (2022).
22. Cao, J. et al. Activation of IL-27 signalling promotes development of postinfluenza pneumococcal pneumonia. *EMBO Mol. Med.* **6**, 120–140 (2014).
23. Xiao, Z. et al. METTL3-mediated m6A methylation orchestrates mRNA stability and dsRNA contents to equilibrate γδ T1 and γδ T17 cells. *Cell Rep.* **42**, 112684 (2023).
24. Sumaria N., Martin S. & Pennington D. J. Constrained TCRγδ-associated Syk activity engages PI3K to facilitate thymic development of IL-17A-secreting γδ T cells. *Science signaling* **14**, (2021).
25. Frascoli, M. et al. Skin γδ T cell inflammatory responses are hard-wired in the thymus by oxysterol sensing via GPR183 and calibrated by dietary cholesterol. *Immunity* **56**, 562–575.e566 (2023).
26. Kobayashi, S. et al. Fatty acid-binding protein 3 controls contact hypersensitivity through regulating skin dermal Vγ4(+) γ/δ T cell in a murine model. *Allergy* **76**, 1776–1788 (2021).
27. Mu, X. et al. Glucose metabolism controls human γδ T-cell-mediated tumor immunosurveillance in diabetes. *Cell. Mol. Immunol.* **19**, 944–956 (2022).
28. Croop, R. et al. Oral rimegepant for preventive treatment of migraine: a phase 2/3, randomised, double-blind, placebo-controlled trial. *Lancet (Lond., Engl.)* **397**, 51–60 (2021).
29. Amaya, F. et al. Induction of CB1 cannabinoid receptor by inflammation in primary afferent neurons facilitates antihyperalgesic effect of peripheral CB1 agonist. *Pain* **124**, 175–183 (2006).
30. Zhang Y., et al. Integrated omics reveal the molecular characterization and pathogenic mechanism of rosacea. *J. Investigative Dermatol.* **144**, 33–42.e2 (2024).
31. Pinho-Ribeiro, F. A. et al. Blocking neuronal signaling to immune cells treats streptococcal invasive infection. *Cell* **173**, 1083–1097.e1022 (2018).
32. Baral, P. et al. Nociceptor sensory neurons suppress neutrophil and gammadelta T cell responses in bacterial lung infections and lethal pneumonia. *Nat. Med.* **24**, 417–426 (2018).
33. Sui, P. et al. Pulmonary neuroendocrine cells amplify allergic asthma responses. *Science (New York, NY)* **360**, eaan8546 (2018).
34. Wallrapp, A. et al. Calcitonin gene-related peptide negatively regulates alarmin-driven type 2 innate lymphoid cell responses. *Immunity* **51**, 709–723.e706 (2019).
35. Lee, S. H. et al. Resolvin D3 controls mouse and human TRPV1-positive neurons and preclinical progression of psoriasis. *Theranostics* **10**, 12111–12126 (2020).
36. Muto, Y. et al. Mast cells are key mediators of cathelicidin-initiated skin inflammation in rosacea. *J. investigative Dermatol.* **134**, 2728–2736 (2014).
37. Meixiong, J., Basso, L., Dong, X. & Gaudenzio, N. Nociceptor-mast cell sensory clusters as regulators of skin homeostasis. *Trends Neurosci.* **43**, 130–132 (2020).
38. Pinho-Ribeiro, F. A. et al. Bacteria hijack a meningeal neuroimmune axis to facilitate brain invasion. *Nature* **615**, 472–481 (2023).
39. Nielsen, M. M., Witherden, D. A. & Havran, W. L. gammadelta T cells in homeostasis and host defence of epithelial barrier tissues. *Nat. Rev. Immunol.* **17**, 733–745 (2017).
40. Mylonas, A. et al. Type I IFNs link skin-associated dysbiotic commensal bacteria to pathogenic inflammation and angiogenesis in rosacea. *JCI Insight* **8**, e151846 (2023).
41. Wang, H. et al. Costimulation of γδTCR and TLR7/8 promotes Vδ2 T-cell antitumor activity by modulating mTOR pathway and APC function. *J. Immunother. Cancer* **9**, e003339 (2021).
42. Deng, Z. et al. Keratinocyte-immune cell crosstalk in a STAT1-mediated pathway: novel insights into rosacea pathogenesis. *Front. Immunol.* **12**, 674871 (2021).

Acknowledgements

This work was supported by the National Natural Science Funds for Distinguished Young Scholars (82225039, J.L.). This work was supported by the National Natural Science Foundation of China (82273557, Y.Z.), and by Natural Sciences Foundation of Hunan province of China (2024JJ5577, Y.Z, 2020JJ5950, Y.Z.) and by National Key Research and Development Program of China (No.2021YFF1201205, J.L.).

Author contributions

J.Li. and Y.Z. designed and conceived the study. Y.Li, and Y.Z. performed data analyses. H.Z., Y.Li., T.Li., Y.Z., and Y.Z. performed mouse experiments and cell experiments. Z.Y. assisted with Tcrd − /− mice. X.Hu. and T.Li. performed wholemount experiments. B.W. and Y.H. contributed to sample collection. X.X. assisted with LC/MS-MS mass spectrometry. J.Li. and Y.Z. provided critical discussion and suggestions. Y.Li, T.Li., H.Z., and Y.Z. prepared the manuscript with input from coauthors.

Competing interests

The authors declare that they have no conflict of interest.

Additional information

Supplementary information The online version contains supplementary material available at https://doi.org/10.1038/s41467-024-50970-1.

Correspondence and requests for materials should be addressed to Yangfan Li or Ji Li.

Peer review information *Nature Communications* thanks Tetsuya Honda, Brian Kim and the other, anonymous, reviewer(s) for their contribution to the peer review of this work. A peer review file is available.